Modeling and Suppression Method for Guided Mode in TC-SAW Devices

Gongbin Tang[1*], Rei Goto[1], and Hiroyuki Nakamura[1*]
[1]Skyworks Solutions, Inc., Kadoma, Osaka 5710050, Japan
[*]E-mail: gongbin.tang@gmail.com, Hiroyuki.Nakamura@skyworksinc.com

Abstract—**In this paper, a modelling and suppression method of the guided mode in high performance temperature compensated surface acoustic wave (TC-SAW) devices is introduced. First, we analyzed the polarizations, acoustic velocity and dispersion characteristics of guided mode, Then, instead of the traditional single-mode COM model, an extended COM model is introduced for analysis of the coupling between the Rayleigh mode and guided mode. This multi-mode COM model can predict the interaction between Rayleigh and guided modes in TC-SAW devices. Last, we verified the effectiveness of this method by a one-port synchronous SAW resonator. This method was very effective in improving the prediction accuracy of the spurious response.**

Keywords—TC SAW; carrier aggression; guided mode; multi-mode COM;

I. INTRODUCTION

Presently, radio frequency (RF) surface acoustic wave (SAW) devices are widely used in modern communication systems thanks to its high performance and low cost. With the growing demand for temperature stability, low loss and wide bandwidth, many novel device structures are raised. Among various innovations, TC-SAW devices, using SiO_2 film on $LiNbO_3$ substrate, have been widely employed in filters and duplexers for applications to the cellular handset market [1]-[13].

Generally speaking, high *Q*, large k^2_{eff} and spurious free are fundamental aspects for SAW resonators to enable high quality filters or multiplexers. 128°YX $LiNbO_3$ is a common wafer applied in TC-SAW devices, where a Rayleigh mode is formed efficiently by the interdigital transducer (IDT). Usually, such device could provide quite satisfying performances even without extreme design considerations. However, with more stringent requirement on device performance, spurious modes, such as transverse type and SH type spurious modes are becoming vital problems for such devices, due to the fact that it will not only introduce in-band spikes, but also deteriorate the passband insertion loss (IL).

Much work has been done to suppress the spurious modes in the vicinity of the passband. In particular, scalar potential theory was employed to study the transverse mode characteristics, and based on this theory, various design methodologies regarding transverse spurious modes suppressions were studied [1]-[13]. To name a few, Dr. Nakamura proposed to use the partial removal of SiO_2 film outside of the active region [9]; while other researchers used a Piston mode operation [10]. As for the SH mode spikes, due to the mutual coupling between the Rayleigh and SH mode [11]-[12], the effect of the SH mode was not considered in the traditional single mode COM model. Recently, some researchers introduced a multi-mode COM model [5], [7]. This model consider the mutual coupling between Rayleigh mode and SH mode, and is quite helpful for analysis and suppression of the spurious modes.

However, for carrier aggregation (CA) applications, it is not enough to only consider the modes in vicinity of the passband. The guided mode, which is substantially confined to the SiO_2 film and has a strong interaction with the Rayleigh mode, should also be analyzed and suppressed [4].

This paper mainly introduces how to analyze the guided mode in TC-SAW devices by using the multi-mode COM model. First, by using FEM/SDA and COMSOL, we analyzed characteristics of the guided mode, including mode polarizations, acoustic velocity and some other basic characteristics. Then, an extended COM model is introduced for analysis of the coupling between the Rayleigh mode and guided mode, by referring to the development of multi-mode COM model used for SH mode analysis. This extended model is also employed for explanation of the mutual coupling between the mentioned two modes. Last, to verify the effectiveness of this method, we fitted the fabricated one-port synchronous SAW resonators by using the proposed model, and the results are quite satisfying.

II. CHARACTERISTIC OF GUIDED MODE IN TC-SAW DEVICES

A. Mode's Analysis

A typical TC-SAW device is over-coated by SiO_2 over layer on top of the IDT, sometimes named as buried interdigital transducer (BIDT) [4]. Figure 1 illustrates a TC-SAW device stack configuration in *zx* plane, where 128°YX $LiNbO_3$ is employed as substrate. SiO_2 is deposited surrounding IDT to improve the temperature coefficient of frequency (TCF).

Based on Fig.1 stack configuration and parameters: h_{IDT}=0.065λ, h_{SiO2}=0.2λ and h_{SiO2}=0.5λ, where λ stands for the resonant wavelength, duty factor (DF) of IDT is 0.45, we calculated the admittances from finite element method and spectral domain analysis (FEMSDA) distributed by Prof. Kenya Hashimoto. Material constants for $LiNbiO_3$ are taken from [8]. Figure 2 (a) and Fig. 2 (b) show the calculated resonator admittance responses.

To understand the characteristics of the modes, we show the corresponding total displacements distributions, where FEM software COMSOL is employed for the calculation.

From Fig.3 (a) and Fig.3 (b), we can see both the Rayleigh mode and SH mode are well confined in the SiO_2 overcoat. By sweeping the SiO_2 overcoat thickness, the temperature coefficient of resonant frequency (TCFs) and effective coupling factor K^2 of the Rayleigh mode are calculated. It is shown though K^2 decreases with SiO_2 thickness, TCFs can be improved ~70ppm/°C with h_{SiO2}=0.5λ. Usually, as shown in Fig.4, for a better TCF, thicker SiO_2 overcoat is preferred. In addition to the Rayleigh and SH mode, another two modes exist ~1.3 times of the resonant frequency f_r. As shown in Fig.2 (b), a plate mode ~4,500m/s, mainly guided by the SiO_2 overcoat, is showing up. Some researchers call it as lamb mode [4] or plate mode [13], we would like to use plate mode in this paper. When h_{SiO2} is smaller than 0.4λ, the plate mode acoustic wave velocity will be close to and even faster than the fast shear bulk acoustic wave velocity, and will radiate into the substrate. The mode profile is shown in Fig.3 (c). Moreover, a bulge with an acoustic velocity from 4,650m/s to 4,750m/s comes up. It is caused by the fast shear bulk acoustic radiation. Compared to the normal bulk acoustic wave cut off shape, the bulge shape is due to the concave shape slowness curve of 128°YX-$LiNbO_3$ substrate in the *zx* plane. Usually, as shown in Fig. 5, when SiO_2 overcoat is becoming thicker, typically h_{SiO2}~0.5λ , the plate mode will have a much higher *Q* than the original state, and the velocity will be decreased. On the contrary, the Rayleigh mode velocity is quite stable, which means a strong waveguide effect of the IDT. Since in the interested region (h_{SiO2}<0.5λ), the plate mode is coupled with the bulge, we would call it as guided mode in this paper.

If filters or multiplexers are designed based on resonators shown in Fig.2, filter transmission performance of neighboring bands will be loaded by unexceptional loss.

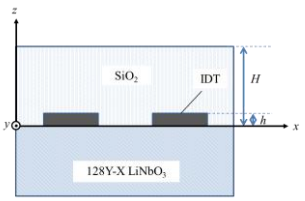

Fig. 1. TC-SAW device geometry in *zx* plane

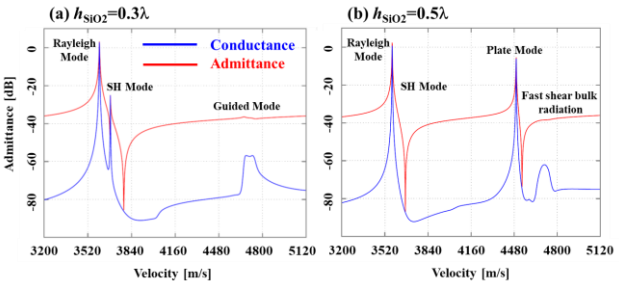

Fig. 2. Simulated admittance and conductance, (a) h_{SiO2}=0.3λ, (b) h_{SiO2}=0.5λ

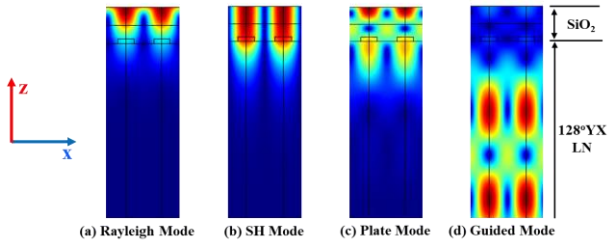

Fig. 3. Simulated total displacement for different modes in TC-SAW, (a) Rayleigh mode, (b) SH mode, (c) Plate mode, (d) Fast shear bulk mode.

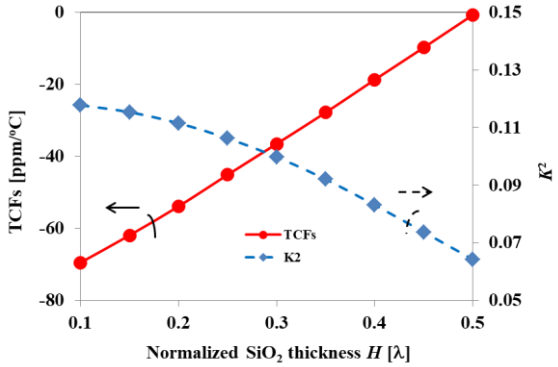

Fig. 4. Dependence of TCFs and K^2 on SiO_2 overcoat thickness

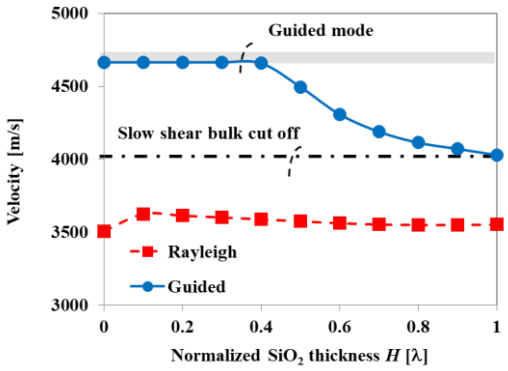

Fig. 5. Dependence of the Rayleigh mode velocity and guided mode velocity on SiO_2 overcoat thickness

B. *Model Description*

We would like to adapt the same methodology as the one used for SH and Rayleigh coupling case. As discussed by Goto [5], we employ the following wave equation for the discussion:

$$\begin{aligned}
\frac{\partial U_1}{\partial x} &= -j\theta_{u1}U_1 + j\kappa_{12}U_2 + j\kappa_{13}U_3 + j\kappa_{14}U_4 + j\alpha_1 \\
\frac{\partial U_2}{\partial x} &= +j\kappa_{21}U_1 + j\theta_{u1}U_2 + j\kappa_{23}U_3 + j\kappa_{24}U_4 - j\alpha_1 \\
\frac{\partial U_3}{\partial x} &= +j\kappa_{31}U_1 + j\kappa_{32}U_2 - j\theta_{u2}U_3 + j\kappa_{34}U_4 + j\alpha_2 \\
\frac{\partial U_4}{\partial x} &= +j\kappa_{41}U_1 + j\kappa_{42}U_2 + j\kappa_{43}U_3 + j\theta_{u2}U_4 - j\alpha_2
\end{aligned} \quad (1)$$

where U_1 and U_2 correspond to the forward and backward propagating Rayleigh modes. U_3 and U_4 correspond to those of the guided modes. κ_{12} and κ_{21} are reflection coefficients for Rayleigh mode and κ_{34} and κ_{43} the guided mode. Except those mentioned coefficients, remaining κ_{ij} stands for mutual coupling coefficients. Besides, α_1 and α_2 stands for the

excitation coefficient of the Rayleigh mode and guided mode respectively.

Based on Fig.1 stack configuration and parameters: h=0.065λ, H=0.4λ, DF=0.45, we extracted the general parameters from FEMSDA as initial input of the multi-mode COM model. Figure 6 illustrates the calculated Brillouin dispersion diagram. As is well known, the mutual coupling between the Rayleigh mode and guided mode is much stronger than that between the Rayleigh mode and SH mode.

There are two existing modes in Fig.6. As for the Rayleigh mode, its short-circuited (SC) dispersion branch, shown in blue line, and the open-circuited (OC) dispersion branch, shown in red line, are both located at the lower frequency side. On the contrary, the guided mode SC and OC branches are located at the higher frequency side. Further insight into Fig.6 shows the Rayleigh mode is resonating at the lower SC stopband edge, while the guided mode is resonating at the higher SC stopband edge. A stopband due to the strong interaction of the Rayleigh and guided mode branch forms in between the two modes. For simplicity, we did not introduce the fast shear bulk radiation this time.

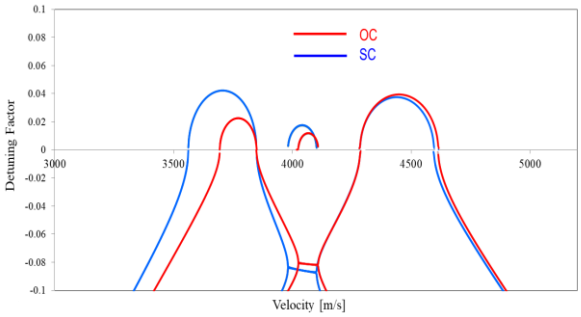

Fig. 6 Dispersion curve for guided mode and Rayleigh mode with mutual coupling

C. Discussion on suppression of the guided mode

As can be seen from the analysis in Fig.6, the guided mode is composed of a plate mode and a fast shear bulk radiation, which is, a leaky plate mode in the interested region (h_{SiO2} ranged from 0.2λ~0.5λ). Based on this, the key point for suppression of the guided mode is divided into two groups: the first is suppression of the plate wave formation, this plate mode can be removed by thinning the SiO_2 overcoat; Usually the SiO_2 overcoat thickness should be less than 0.5λ, where the plate mode is radiating into the substrate; Moreover, some researchers tried to shift down the fast shear bulk acoustic wave in order to radiate the plate mode into the substrate. This is done by rotating the Euler angle in low-cut TC-SAW cases, where acoustic velocity of the fast shear bulk wave decreases with Euler angle φ and ψ [6]. However, as for 128°YX-LN families, the author failed to find a satisfying cut to serve this purpose.

On the other hand, the second method can serve the CA purpose well; this method is shifting downwards the Rayleigh mode rather than suppression of the guided mode. This idea is based on the fact that the guided mode is not sensitive to the IDT mass loading effect, while Rayleigh mode is to the contrary. As can be seen from Fig.7, the Rayleigh mode acoustic wave velocity decreases from ~3800m/s to ~3400m/s when h_{IDT} changes from 0.01 to 0.11. We can adjust the IDT film thickness and pitch comprehensively, to move the guided mode out of the interested regions.

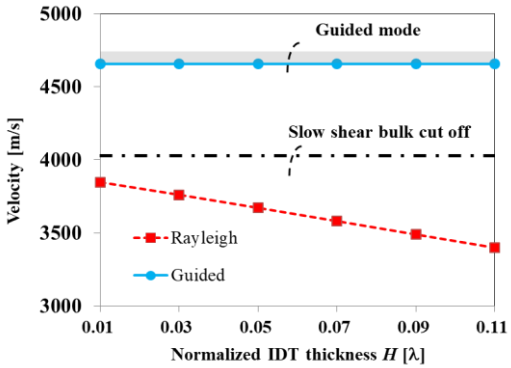

Fig. 7 Dependence of the Rayleigh mode velocity and guided mode velocity on IDT thickness

III. Experimental Verification

A. One-port Synchronous Resonator

To validate the effectiveness of this model, we fabricated one port synchronous resonators on 128°YX-$LiNbO_3$ substrate with the stack configuration shown in Fig. 1 and geometry parameters used in part 2. As shown in Fig. 8, although loss is not accurately matched, the multi-mode COM model agree with the experimental result quite well. The disagreement around Rayleigh mode anti-resonant frequency f_a is due to SH mode responses and Rayleigh transverse modes, while the one after guided mode f_a is due to bulk radiation.

As we expected, the longitudinal ripples of the Rayleigh mode and the guided mode are located below/above the corresponding f_r, this verified the location of f_r is at the lower/upper SC stopband edge, for the two modes. It is interesting to notify that when frequency is higher than the Rayleigh mode upper stopband edge, capacitance for the resonator changed, which may be caused by change of the electric field distribution.

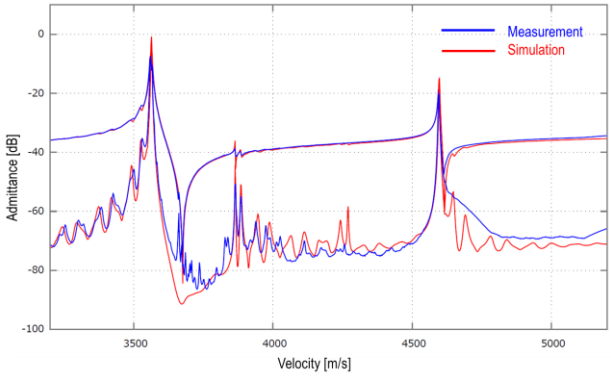

Fig. 8 Experimental verification of the multi-mode COM model for guided mode analysis

IV. Conclusions

In this paper, we applied the multi-mode COM model for analysis of TC-SAW devices with strong mutual coupling between the Rayleigh mode and the guided mode.

First, the basic characteristics of TC-SAW device are analyzed by FEM. Admittance curves and total displacement distributions are calculated to show the definition of the guided mode. As a result, we realize that the usually named guided mode is a coupled mode between a plate mode and the fast shear bulk acoustic wave, while the plate mode exists due to thicker SiO_2 overcoat.

Then, by using the multi-mode COM model proposed initially for consideration of the mutual coupling between the Rayleigh mode and SH mode, we could successfully simulate the mutual coupling between the Rayleigh mode and the guided mode. By fitting to a dispersion curve calculated by FEMSDA, we realize both the Rayleigh mode and SH mode branches agree well and the mutual coupling between them can also be traced by using the multimode COM model. Moreover, during fitting our model to the dispersion curves, we realized the mutual coupling between the Rayleigh mode and the guided mode is much stronger than that between the Rayleigh mode and the SH mode. Based on the FEM simulation, the suppression methods of the guided mode is also discussed. Thinner SiO_2 is preferred, thicker IDT is also helpful for less guided mode loading effects.

To verify the multimode COM model, a comparison with the one synchronous resonator measurement was compared. The comparison shows the guided mode spurious response can be predicted by the multi-mode model.

References

[1] K. Yamanouchi, S. Hayama, "SAW Properties of SiO_2/128°Y-X $LiNbO_3$ Structure Fabricated by Magnetron Sputtering Technique", IEEE Trans. on Sonics and Ultrason., SU-31, (1984) pp. 51-57.

[2] M. Kadota, "High Performance and Miniature Surface Acoustic Wave Devices with Excellent Temperature Stability Using High Density Metal Electrodes," IEEE Ultrasonics Symp., pp. 496-506 (2007).

[3] Y. Nakai, T. Nakao, K. Nishiyama, and M. Kadota, "Surface Acoustic Wave Duplexer Composed of SiO2 film with Convex and Concave on Cu-electrodes/LiNbO3 Structure," IEEE Ultrasonics Symp., pp. 1580-1583 (2008).

[4] B. Abbott, A. Chen, T. Daniel, K. Gamble, T. Kook, M. Solal, K. Steiner, R. Aigner, S. Malocha, C. Hella, M. Gallagher, and J. Kuypers, "Temperature compensated saw with high quality factor", Proc. IEEE Ultrasonics (2017), p. 1.

[5] R. Goto, J. Fujiwara, H. Nakamura, and K. Hashimoto, "Multimode coupling of modes model for spurious responses on SiO_2/$LiNbO_3$ substrate", Jpn. J. Appl. Phys. 57, 07LD20 (2018).

[6] R. Goto, J. Fujiwara, H. Nakamura, T. Tsurunari, H. Nakanishi,and Y. Hamaoka, "Study of spurious response near the fast shear wave in SiO_2/Al/$LiNbO_3$ structure", Jpn. J. Appl. Phys. 57, 07LD20 (2018).

[7] Y. Huang, J. Bao, X. Li, B. Zhang, G. Tang, T. Omori, K. Hashimoto, "Influence of coupling between Rayleigh and SH SAWs on rotated Y-eut $LiNbO_3$ to their eleetromeehanieal coupling faetor", IEEE transactions on Ultrasonics, Ferroelectrics, and Frequency Control, 65(10), (2018) 1905-1913.

[8] G. Kovacs, M. Anhorn, H. E. Engan, G. Visintini, and C. C. W. Ruppel, Improved material constants for $LiNbO_3$ and $LiTaO_3$, Proc. 1990 IEEE Ultrasonics Symp., pp. 435-438, 1990.

[9] H. Nakamura, H. Nakanishi, R. Goto, and K. Hashimoto, "Suppression Mechanism of Transverse-Mode Spurious Responses in SAW Resonators on a SiO_2/Al/$LiNbO_3$ Structure," in Proc. IEEE Intl. Ultrasonics Symp., Orlando, FL, Oct. 2011, pp. 1–4.

[10] M. Solal, J. Gratier, R. Aigner, K. Gamble, B. Abbott, T. Kook, A. Chen and K. Steiner,"Transverse modes suppression and loss reduction for buried electrodes SAW devices," Proc. IEEE Ultrason. Symp. (2010) pp. 624-628.

[11] V. Plessky, P. Turner, N. Fenzi and V. Grigorievsky, "Interaction between the Rayleigh-type SAW and the SH-wave in a periodic grating on a 128°-LN substrate," *2010 IEEE International Ultrasonics Symposium*, San Diego, CA, 2010, pp. 167-170.

[12] N. F. Naumenko and B. P. Abbott, "Transformation of acoustic waves in periodic metal grating sandwiched between piezoelectric and dielectric," in *IEEE Transactions on Ultrasonics, Ferroelectrics, and Frequency Control*, vol. 58, no. 10, pp. 2181-2187, October 2011.

[13] J. Koskela , V. Plessky, B. Willemsen, P. Turner, B. Hammond, and N. Fenzi, "Hierarchical Cascading Algorithm for 2-D FEM Simulation of Finite SAW Devices," IEEE Trans. Ultrason. Ferroelectr. Freq. Control, vol.65,no.10,pp.1933–1942,Jul.2018.